CHAPTER TEN

Environmental fluid dynamics of tidal bores: Theoretical considerations and field observations

Hubert Chanson
Professor in Civil Engineering, The University of Queensland, Brisbane, Australia

ABSTRACT

A tidal bore is a series of waves propagating upstream as the tidal flow turns to rising in a river mouth during the early flood tide. The formation of the bore occurs is linked with a macro-tidal range exceeding 4.5 to 6 m, a funnel shape of the river mouth and estuarine zone to amplify the tidal range. After formation of the bore, there is an abrupt rise in water depth at the bore front associated with a flow singularity in terms of water elevation, and pressure and velocity fields. The application of continuity and momentum principles gives a complete solution of the ratio of the conjugate cross-section areas as a function of the upstream Froude number. The effects of the flow resistance are observed to decrease the ratio of conjugate depths for a given Froude number. The field observations show that the tidal bore passage is associated with large fluctuations in water depth and instantaneous velocity components associated with intense turbulent mixing. The interactions between tidal bores and human society are complex. A tidal bore impacts on a range of socio-economic resources, encompassing the sedimentation of the upper estuary, the impact on the reproduction and development of native fish species, and the sustainability of unique eco-systems. It can be a major tourism attraction like in North America, Far East Asia and Europe, and a number of bores are surfed with tidal bore surfing competitions and festivals. But a tidal bore is a massive hydrodynamic shock which might become dangerous and hinder the local traffic and economical development.

10.1 INTRODUCTION

A tidal bore is a series of waves propagating upstream as the tidal flow turns to rising. It is an unsteady flow motion generated by the rapid rise in free-surface elevation at the river mouth during the early flood tide. The formation of a bore occurs when the tidal range exceeds 4.5 to 6 m and the funnel shape of both river mouth and lower estuarine zone amplifies the tidal wave. The driving process is the large tidal amplitude and its amplification in the estuary. After formation of the bore, there is an abrupt rise in water depth at the bore front associated with a flow singularity in terms of water elevation, and pressure and velocity fields. The tidal bore is a positive surge also called hydraulic jump in translation. Figures 10.1 to 10.5 illustrate some tidal bores in China, France and Indonesia. Pertinent accounts include Moore (1888), Darwin (1897), Moule (1923), and Chanson (2011). The existence of the tidal bore is based upon a fragile hydrodynamic balance between the tidal amplitude, the freshwater river flow conditions and the river channel bathymetry, and this balance may be easily disturbed by changes in boundary conditions and freshwater inflow (Chanson 2011). A number of man-made interferences led to the disappearance of tidal bores in France, Canada, Mexico for example. While the fluvial navigation gained in safety, the ecology of the estuarine systems was affected adversely, e.g. with the disappearance of native fish species. Natural events do also affect tidal bores: e.g., the 1964 Alaska earthquake on the Turnagain and Knik Arms bores, the 2001 flood of Ord River (Australia), the combination of storm surge and spring tide in Bangladesh in November 1970.

A related process is the tsunami-induced bore. When a tsunami wave propagates in a river, its leading edge is led by a positive surge. The tsunami-induced bore may propagate far upstream. Some tsunami-induced river bores were observed in Hawaii in 1946, in Japan

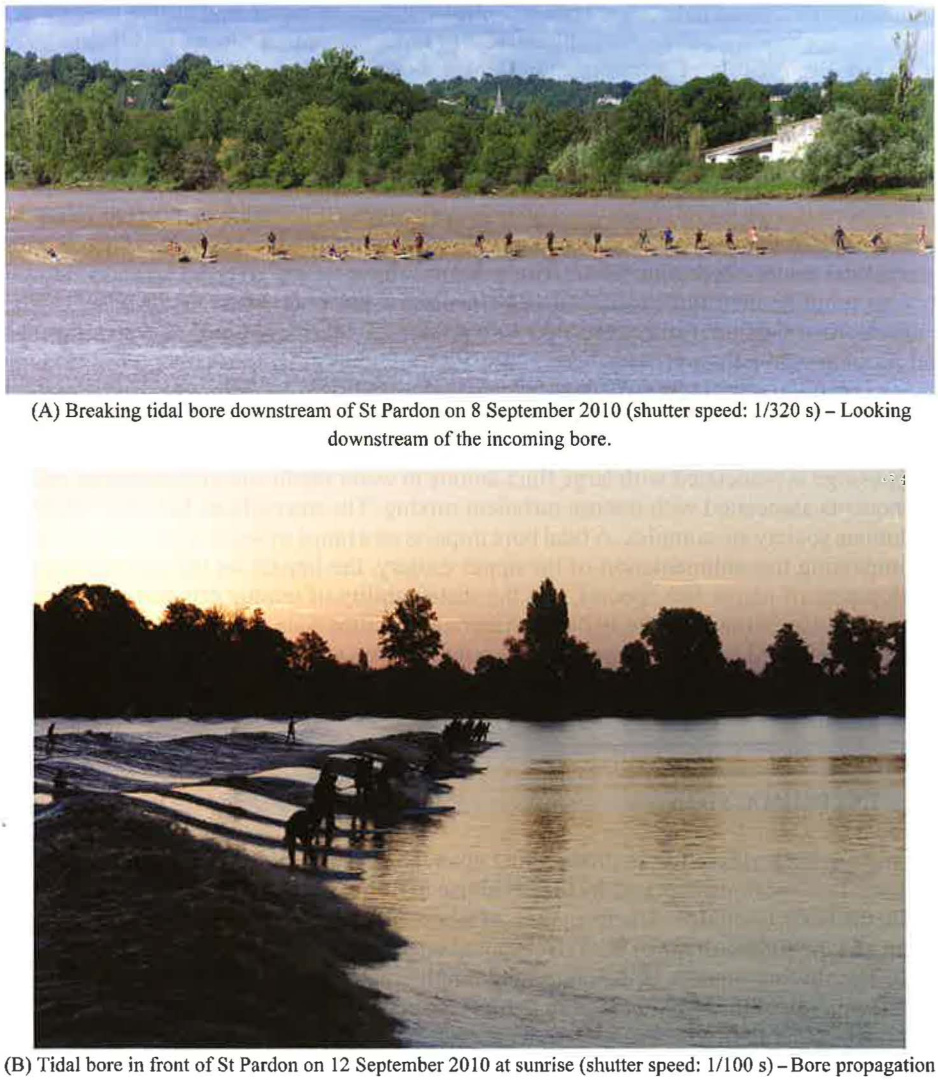

(A) Breaking tidal bore downstream of St Pardon on 8 September 2010 (shutter speed: 1/320 s) – Looking downstream of the incoming bore.

(B) Tidal bore in front of St Pardon on 12 September 2010 at sunrise (shutter speed: 1/100 s) – Bore propagation from left to right.

Figure 10.1. Tidal bore of the Dordogne River (France).

(C) Undular tidal bore in front of St Sulpice de Faleyrens on 19 June 2011 evening (shutter speed: 1/500 s) (Courtesy of Mr and Mrs Chanson) – Bore propagation from right to left.

Figure 10.1. *Continued.*

in 1983, 2001, 2003 and 2011, and even in the River Yealm in United Kingdom on 27 June 2011. During the 11 March 2011 tsunami catastrophe in Japan, tsunami-induced bores were observed in several rivers in north-eastern Honshu and as far s North-America.

After a brief introduction on tidal bores, some basic theoretical developments are developed. Then some recent field observations are presented and discussed. The results are challenging since the propagation of tidal bores is associated with sediment scour, strong mixing and suspended sediment advection upstream. It will be shown that the hydrodynamics of tidal bores remains a challenge to engineers and scientists because of the unsteady nature and sharp discontinuity of the flow.

10.2 THEORETICAL CONSIDERATIONS

10.2.1 Presentation

A tidal bore is characterised by a sudden rise in free-surface elevation and a discontinuity of the pressure and velocity fields. In the system of reference following the bore front, the integral form of the continuity and momentum equations gives a series of relationships between the flow properties in front of and behind the bore (Rayleigh, 1914; Henderson, 1966; Liggett, 1994):

$$(V_1 + U) \times A_1 = (V_2 + U) \times A_2 \tag{10.1}$$

(A) Tidal bore at Podensac on 11 September 2010 morning (shutter speed: 1/320 s) – Looking downstream at the incoming tidal bore.

(B) Undular tidal bore upstream of Podensac on 16 August 2011 evening (shutter speed: 1/2,000 s) (Courtesy of Isabelle Borde) – Bore propagation from left to right.

Figure 10.2. Tidal bore of the Garonne River (France).

$$\rho \times (V_1 + U) \times A_1 \times (\beta_1 \times (V_1 + U) - \beta_2 \times (V_2 + U)) = \iint_{A_2} P \times dA - \iint_{A_1} P \times dA + F_{fric} - W \times \sin\theta \tag{10.2}$$

where V is the flow velocity and U is the bore celerity for an observer standing on the bank (Fig. 10.6), ρ is the water density, g is the gravity acceleration, A is the channel

Figure 10.3. Tidal bore of the Kampar River (Indonesia) in September 2010 (Courtesy of Antony Colas) – Bore propagation from right to left.

Figure 10.4. Tidal bore of the Qiantang River(China) at Yanguan on 23 July 2009 (shutter speed: 1/500 s) (Courtesy of Jean-Pierre Girardot) – The tidal range was 4 m – Bore propagation from left to right.

(A) Breaking bore in front of Pointe du Grouin du Sud on 19 October 2008 morning (shutter speed: 1/640 s) – Bore propagation from right to left.

(B) Breaking tidal bore downstream of Pointe du Grouin du Sud on 24 September 2010 evening (shutter speed: 1/125 s) – Bore propagation from right to left.

Figure 10.5. Tidal bore of the Sélune River (France).

cross-sectional area measured perpendicular to the main flow direction, β is a momentum correction coefficient or Boussinesq coefficient, P is the pressure, F_{fric} is the flow resistance force, W is the weight force, θ is the angle between the bed slope and horizontal, and the subscripts 1 and 2 refer respectively to the initial flow conditions and the flow conditions immediately after the tidal bore. Note that U is positive for a tidal bore (Fig. 10.6).

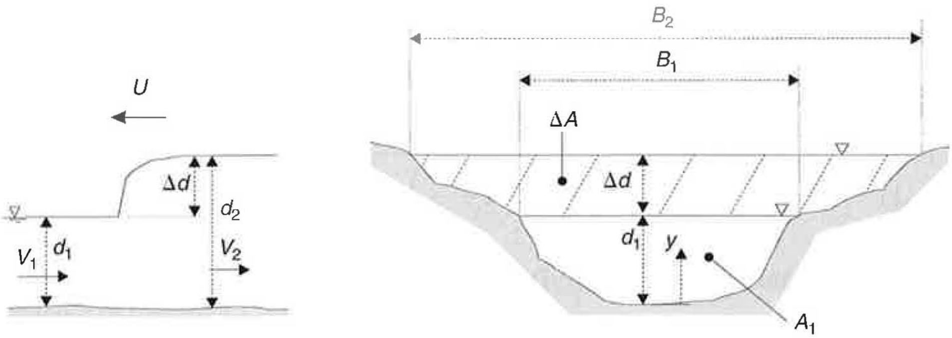

Figure 10.6. Definition sketch of a tidal bore propagating upstream.

10.2.2 Momentum considerations

The continuity and momentum equations provide some analytical solutions within some basic assumptions. First let us neglect the flow resistance and the effect of the velocity distribution ($\beta_1 = \beta_2 = 1$) and let us assume a flat horizontal channel ($\sin\theta \approx 0$). The momentum principle becomes:

$$\rho \times (V_1 + U) \times A_1 \times (V_1 - V_2) = \iint_{A_2} P \times dA - \iint_{A_1} P \times dA \tag{10.3}$$

In the system of reference in translation with the bore, the rate of change of momentum flux equals the difference in pressure forces. The latter may be expressed assuming a hydrostatic pressure distribution in front of and behind the tidal bore. The net pressure force resultant consists of the increase of pressure $\rho \times g \times (d_2 - d_1)$ applied to the initial flow cross-section area A_1 plus the pressure force on the area $\Delta A = A_2 - A_1$. This latter term equals:

$$\int_{A_1}^{A_2}\!\!\int \rho \times g \times (d_2 - y) \times dA = \frac{1}{2} \times \rho \times g \times (d_2 - d_1)^2 \times B' \tag{10.4}$$

where y is the distance normal to the bed, d_1 and d_2 are the flow depths in front of and behind the bore (Fig. 10.6), and B' is a characteristic free-surface width. It may be noted that $B_1 < B' < B_2$ where B_1 and B_2 are the upstream and downstream free-surface widths

Another characteristic free-surface width B is defined as:

$$B = \frac{A_2 - A_1}{d_2 - d_1} \tag{10.5}$$

The equation of conservation of mass may be expressed as:

$$V_1 - V_2 = (V_1 + U) \times \frac{A_2 - A_1}{A_2} \tag{10.6}$$

The combination of the equations of conservation of mass and momentum (Eq. (10.3) and (10.6)) yields to the following expressions:

$$U + V_1 = \sqrt{\frac{1}{2} \times \frac{g \times A_2}{A_1 \times B} \times \left(\left(2 - \frac{B'}{B}\right) \times A_1 + \frac{B'}{B} \times A_2\right)} \tag{10.7}$$

$$V_1 - V_2 = \sqrt{\frac{1}{2} \times \frac{g \times (A_2 - A_1)^2}{B \times A_1 \times A_2}\left(\left(2 - \frac{B'}{B}\right) \times A_1 + \frac{B'}{B} \times A_2\right)} \tag{10.8}$$

After transformation, Equation (10.7) may be rewritten in the form:

$$Fr_1 = \sqrt{\frac{1}{2} \times \frac{A_2}{A_1} \times \frac{B_1}{B} \times \left(\left(2 - \frac{B'}{B}\right) + \frac{B'}{B} \times \frac{A_2}{A_1}\right)} \tag{10.9}$$

where Fr_1 is the tidal bore Froude number defined as:

$$Fr_1 = \frac{U + V_1}{\sqrt{g \times \frac{A_1}{B_1}}} \tag{10.10}$$

Equation (10.10) defines the Froude number for an irregular channel based upon momentum considerations. Interestingly the same expression may be derived from energy considerations (Henderson, 1966; Chanson, 2004).

Altogether Equation (10.9) provides an analytical solution of the tidal bore Froude number as a function of the ratios of cross-sectional areas A_2/A_1, and of characteristic widths B'/B and B_1/B. The effects of the celerity are linked implicitly with the initial flow conditions, including for a fluid initially at rest ($V_1 = 0$). Equation (10.9) may be rewritten to express the ratio of conjugate cross-section areas A_2/A_1 as a function of the upstream Froude number:

$$\frac{A_2}{A_1} = \frac{1}{2} \times \frac{\sqrt{\left(2 - \frac{B'}{B}\right)^2 + 8 \times \frac{\frac{B'}{B}}{\frac{B_1}{B}} \times Fr_1^2} - \left(2 - \frac{B'}{B}\right)}{\frac{B'}{B}} \tag{10.11}$$

which is valid for any tidal bore in an irregular flat channel (Fig. 10.6). The effects of channel cross-sectional shape are taken into account through the ratios B'/B and B_1/B.

Limiting cases

In some particular situations, the cross-sectional shape satisfies the approximation $B_2 \approx B \approx B' \approx B_1$: for example, a channel cross-sectional shape with parallel walls next to the waterline or a rectangular channel. In that case, Equations (10.7) and (10.8) may be simplified into:

$$U + V_1 = \sqrt{\frac{1}{2} \times \frac{g}{A_1} \times \frac{(A_1 + A_2) \times A_2}{B}} \qquad B_2 \approx B \approx B' \approx B_1 \tag{10.12}$$

$$V_1 - V_2 = \sqrt{\frac{1}{2} \times \frac{g \times (A_1 + A_2) \times (A_2 - A_1)^2}{B \times A_1 \times A_2}} \qquad B_2 \approx B \approx B' \approx B_1 \tag{10.13}$$

The above solution is close to the development of Lighthill (1978). Equation (10.12) may be expressed as the ratio of conjugate cross-section areas as a function of the upstream Froude number Fr_1:

$$\frac{A_2}{A_1} = \frac{1}{2} \times \left(\sqrt{1 + 8 \times Fr_1^2} - 1\right) \qquad B_2 \approx B \approx B' \approx B_1 \tag{10.14}$$

This last equation yields to the Bélanger equation for a rectangular horizontal channel in absence of friction:

$$\frac{d_2}{d_1} = \frac{1}{2} \times \left(\sqrt{1 + 8 \times Fr_1^2} - 1\right) \qquad \text{Rectangular channel} \tag{10.15}$$

Application

Several field observations of tidal bores were documented with detailed hydrodynamic and bathymetric conditions. The data are summarised in Table 10.1. Figure 10.5B shows the Sélune River channel during the field study on 24 September 2010 and the photograph highlights the wide and flat cross-sectional shape. Despite the range of channel cross-sectional shapes, the data indicated that the approximation $B_1 < B' < B < B_2$ held on average (Table 10.1).

The upstream Froude number was calculated using Equation (10.10) based upon the field measurements of velocity and bore celerity, and the data are summarised in Figure 10.7. Figure 10.7 presents the upstream Froude number as a function of the ratio of conjugate cross-section areas. The data are compared with Equation (10.11) for irregular channel cross-sections and with Equation (10.14) for channel cross-sectional shapes with parallel walls next to the waterline. The results highlight the effects of the irregular cross-section and illustrate that Equation (10.14) is not appropriate in an irregular channel like a natural estuarine system.

Further the definition of the Froude number Fr_1 (Eq. (10.10)) differs from the traditional approximation $V_1/(g \times d_1)^{0.5}$. For the data listed in Table 10.1 and shown in Figure 10.7, the difference varied between 12% and 74%!

10.2.3 Discussion: effects of flow resistance

In presence of some boundary friction and drag losses, the flow resistance force is non-zero and the equation of conservation of momentum may be solved analytically for a flat horizontal channel. The combination of the equations of conservation of mass and momentum yields:

$$U + V_1 = \sqrt{\frac{1}{2} \times \frac{g \times A_2}{A_1 \times B} \times \left(\left(2 - \frac{B'}{B}\right) \times A_1 + \frac{B'}{B} \times A_2\right) + \frac{A_2}{A_2 - A_1} \times \frac{F_{fric}}{\rho \times A_1}} \tag{10.16}$$

Table 10.1. Hydrodynamics and bathymetric properties of tidal bores.

River	Bore	Date	Ref.	d_1 (m)	U (m/s)	Fr_1 (m)	$d_2 - d_1$	A_2/A_1
Dee	Breaking	2/07/03	[SFW04]	1.50	4.70	1.04	0.28	1.13
Daly	Undular	6/09/03	[WWSC04]	0.72	4.10	1.79	0.45	1.80
Garonne	Undular	10/08/10	[CLSR10]	1.77	4.49	1.30	0.50	1.37
Garonne	Undular	11/09/10	[CLSR10]	1.81	4.20	1.20	0.46	1.33
Sélune	Breaking	24/09/10	[MCS10]	0.38	2.00	2.35	0.34	6.19
Sélune	Breaking	25/09/10	[MCS10]	0.33	1.96	2.48	0.41	9.79

River	Bore	Date	B_2/B_1	B/B_1	B'/B_1	A_2/A_1 Eq. (10.11)
Dee	Breaking	2/07/03	1.013	1.007	1.001	1.052
Daly	Undular	6/09/03	1.066	1.030	1.085	2.09
Garonne	Undular	10/08/10	1.083	1.042	1.018	1.44
Garonne	Undular	11/09/10	1.076	1.032	1.021	1.30
Sélune	Breaking	24/09/10	3.37	2.33	1.92	4.92
Sélune	Breaking	25/09/10	3.53	2.33	1.98	5.18

Notes: d_1: initial water depth at sampling location; *Italic data*: incomplete data; [SFW04]: Simpson *et al.* (2004); [WWSC04]: Wolanski *et al.* (2004); [CLSR10]: Chanson *et al.* (2010); [MCS10]: Mouazé *et al.* (2010).

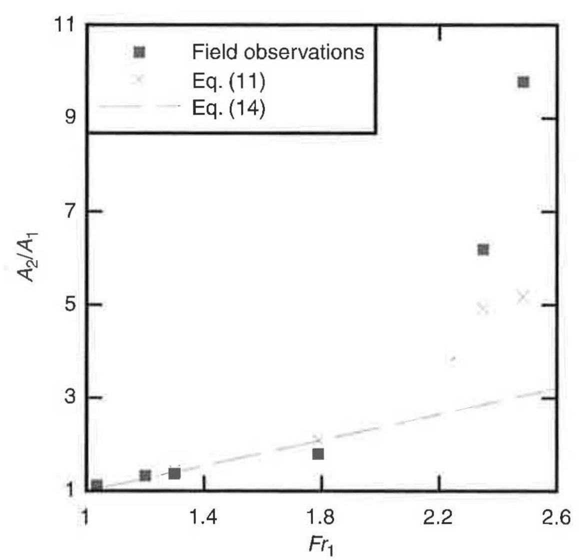

Figure 10.7. Momentum application to tidal bores in irregular cross-section channels – Comparison between field observations (Table 10.1) and Equations (10.11) and (10.14).

$$V_1 - V_2 = \sqrt{\frac{1}{2} \times \frac{g \times (A_2 - A_1)^2}{B \times A_1 \times A_2} \left(\left(2 - \frac{B'}{B} \right) \times A_1 + \frac{B'}{B} \times A_2 \right) + \frac{A_2}{A_2 - A_1} \frac{F_{fric}}{\rho \times g \times \frac{A_1^2}{B}}} \quad (10.17)$$

Equations (10.16) and (10.17) are the extension of Equations (10.7) and (10.8) in presence of flow resistance. The results may be transformed into:

$$Fr_1 = \sqrt{\frac{1}{2} \times \frac{A_2}{A_1} \times \frac{B_1}{B} \times \left(\left(2 - \frac{B'}{B} \right) + \frac{B'}{B} \times \frac{A_2}{A_1} \right) + \frac{A_2}{A_2 - A_1} \times \frac{F_{fric}}{\rho \times g \times \frac{A_1^2}{B}}} \quad (10.18)$$

The result (Eq. (10.18)) gives a relationship between the tidal bore Froude number, the ratio of the conjugate cross-section areas A_2/A_1 and the flow resistance force in flat channels of irregular cross-sectional shape. Figure 10.8 illustrates the effects of bed friction on the hydraulic jump properties for a irregular channel corresponding to the bathymetric conditions of the Sélune River listed in Table 10.1.

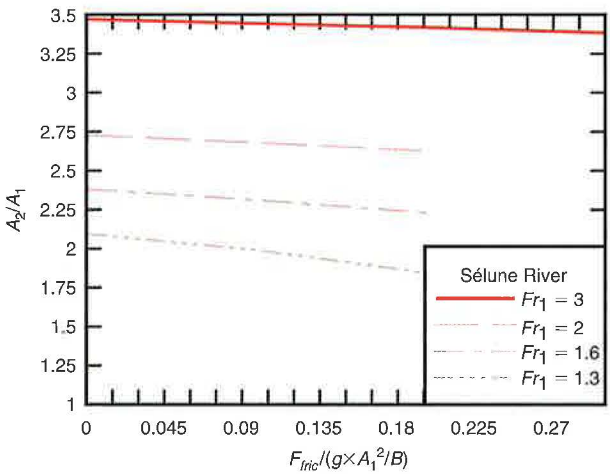

Figure 10.8. Effect of flow resistance on the tidal bore properties in an irregular channel.

The theoretical developments imply a smaller ratio of the conjugate depths d_2/d_1 with increasing flow resistance. The finding is consistent with laboratory data (for example Leutheusser and Schiller, 1975). It is more general and applicable to any irregular channel cross-sectional shape. Importantly the results highlighted that the effects of flow resistance decrease with increasing Froude number and become negligible for Froude numbers greater than 2 to 3 depending upon the cross-sectional properties (Fig. 10.8).

10.3 FIELD OBSERVATIONS

10.3.1 Presentation

When a tidal bore is formed, the flow properties immediately upstream and downstream of its front must satisfy the principles of continuity and momentum (section 10.2). Theoretical considerations demonstrate that a key dimensionless parameter is the tidal bore Froude number defined as:

$$Fr_1 = \frac{U + V_1}{\sqrt{g \times \frac{A_1}{B_1}}} \tag{10.10}$$

Fr_1 characterises the strength of the bore. If the Froude number Fr_1 is less than unity, the tidal bore cannot form. For a Froude number between 1 and 1.5 to 1.8, the bore is followed by a train of quasi-periodic secondary waves called whelps or undulations. This type of bore is the undular non-breaking bore illustrated in Figures 10.1, 10.2 and 10.9. The free-surface properties of undular tidal bores were investigated for more than a century (Boussinesq, 1877; Lemoine, 1948; Chanson, 2010). A recent review showed that the rate of energy dissipation is small to negligible, while the approximation of hydrostatic pressure is inaccurate. The free-surface profile present a pattern somehow comparable to the sinusoidal and cnoidal wave functions, although neither captures the fine details of the undulation shape and asymmetrical wave profile (Chanson, 2010). Field and laboratory data showed a maximum in wave amplitude and steepness for $Fr_1 = 1.3$ to 1.4 corresponding to the apparition of some breaking at the first wave crest.

For larger Froude numbers, the bore tidal has a breaking front with a marked roller. Examples are shown in Figures 10.3 to 10.5.

Figure 10.9. Undular tidal bore the Garonne River on 10 September 2010 at Arcins (shutter speed: 1/125 s) – Bore propagation from right to left – The surfer in the background rides the bore front.

Table 10.2. Detailed field measurements of turbulent velocity in tidal bores.

River	Country	Bore type	Date	Ref.	Instrument	Sampling rate (Hz)
Dee	UK	Breaking	2/07/03	[SFW04]	ADCP (1.2 MHz)	1
Daly	Australia	Undular	6/09/03	[WWSC04]	ADCP Nortek Aquadopp	2
Garonne	France	Undular	10/08/10	[CLSR10]	ADV Nortek Vector (6 MHz)	64
Garonne	France	Undular	11/09/10	[CLSR10]	ADV Nortek Vector (6 MHz)	64
Sélune	France	Breaking	24/09/10	[MCS10]	ADV Nortek Vector (6 MHz)	64
Sélune	France	Breaking	25/09/10	[MCS10]	ADV Nortek Vector (6 MHz)	64

River	Bore	Date	d_1 (m)	U (m/s)	Fr_1	z (m)	z/d_1
Daly	Undular	2/07/03	1.50	4.70	1.04	*0.75*	0.5
Dee	Breaking	6/09/03	0.72	4.10	1.79	0.55	0.76
Garonne	Undular	10/08/10	1.77	4.49	1.30	0.81 m below surface	0.54(*)
Garonne	Undular	11/09/10	1.81	4.20	1.20	0.81 m below surface	0.55(*)
Sélune	Breaking	24/09/10	0.38	2.00	2.35	0.225	0.59
Sélune	Breaking	25/09/10	0.33	1.96	2.48	0.10	0.30

Notes: d_1: initial water depth at sampling location; *Italic data*: incomplete data; z: sampling elevation above bed; [SFW04]: Simpson *et al.* (2004); [WWSC04]: Wolanski *et al.* (2004); [CLSR10]: Chanson *et al.* (2010); [MCS10]: Mouazé *et al.* (2010); (*): immediately prior to bore passage.

All the field observations highlighted the intense turbulence generated by the advancing bore (Fig. 10.1 to 10.5). Moule (1923) reported a description of the Qiantang River bore (China) from the 13th century: "*when the wave [or tide] comes it is steep as a mountain, roaring like thunder, a horizontal flying bank of water [or ice] and sidelong shooting precipice of snow plunging and leaping in a dreadful manner*". Bazin (1865) described the destructive power of the Hoogly River tidal bore in India: "*the tidal bore creates a 4 to 5 m high wall of water, and advances with a great noise announcing the flood tide; it entrains upstream all the floating debris and sinks the small boats on the shoals and in shallow waters*". La Condamine (1745) documented the impact of the passage of the Amazon River bore: "*One can see a wall of water of 4 to 5 m in height, then another, then a third one and sometimes a fourth one, that comes close together, and that occupies all the width of the channel; this bore advanced very rapidly, breaks and destroy everything*". A further illustration of intense turbulence is the number of field work incidents, encompassing studies in the Dee River, Rio Mearim, Daly River and Sélune River. In the Rio Mearim "*one sawhorse and instrument tumbled along the bottom for 1.4 km with currents exceeding 3 m·s^{-1}, was buried in a sand bank, and had to be abandoned*" (Kjerve and Ferreira, 1993). In the Sélune River, "*the field study experienced a number of problems and failures. About 40 s after the passage of the bore, the metallic frame started to move. The ADV support failed completely 10 minutes after the tidal bore*" (Mouazé et al., 2010).

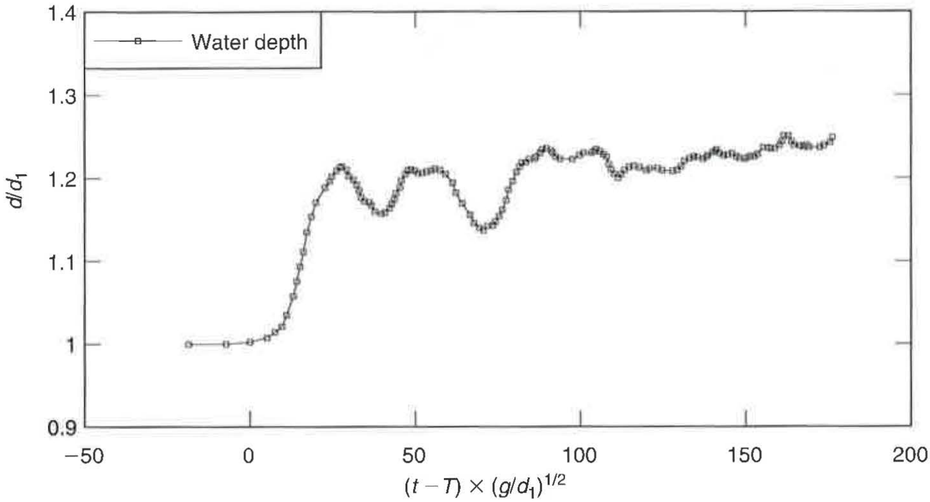

(A) Undular tidal bore of the Daly Riveron 2 July 2001.

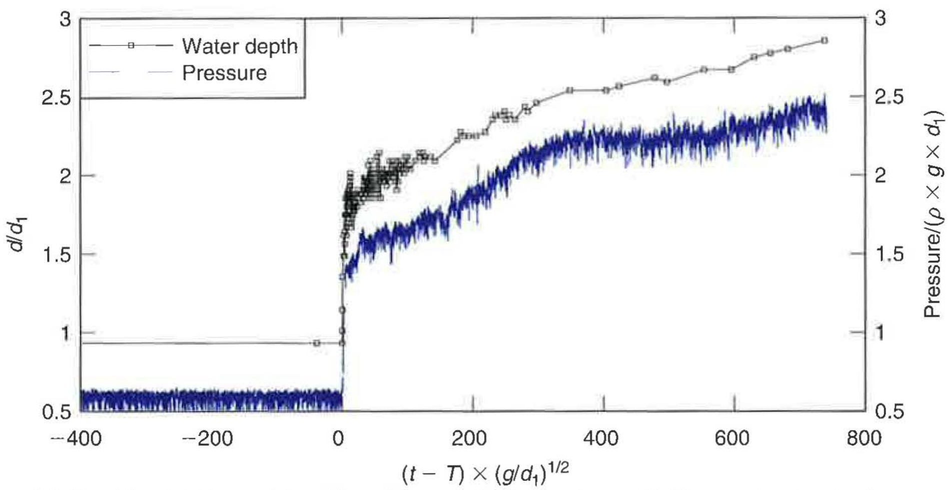

(B) Breaking tidal bore of the Sélune River on 24 September 2010-Observed water depth and pressure sampled at 0.225 m above bed.

Figure 10.10. Time-variations of water depth and free-surface discontinuity across a tidal bore.

Some recent free-surface and turbulent velocity measurements were conducted in the field with detailed temporal and spatial resolutions (Table 10.2). The data provide an unique characterisation of the unsteady turbulent field and mixing processes. Table 10.2 summarises the basic flow conditions and includes details on the instrumentation. The basic outcomes are summarised in this section.

10.3.2 Field observations

The propagation of a tidal bore is associated with a sudden rise in free-surface elevation. Basically the passage of the tidal bore creates a sudden discontinuity in terms of the flow depth followed by large, long-lasting fluctuations of the free-surface behind the bore front.

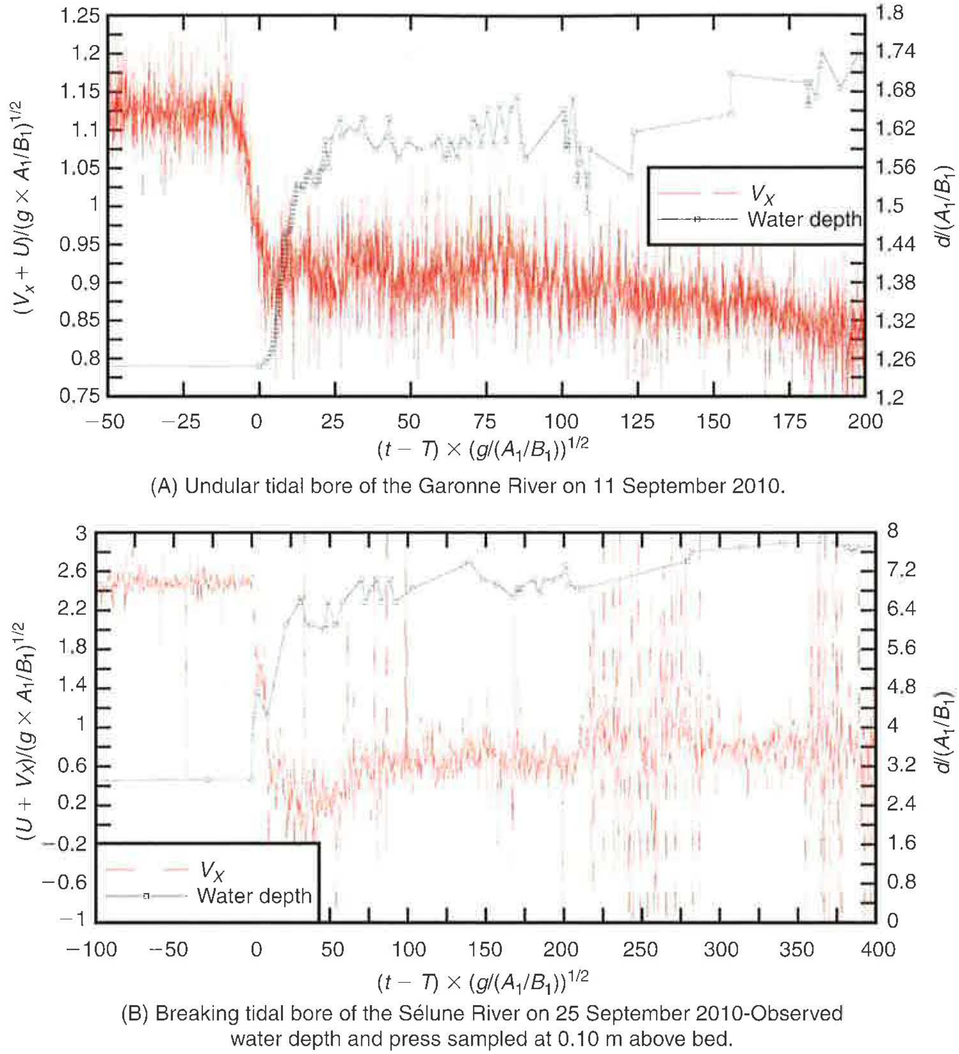

Figure 10.11. Time-variations of the dimensionless water depth and longitudinal velocity during a tidal bore passage.

Typical field observations are presented in Figure 10.10 for an undular and breaking bore. Figure 10.10 shows the dimensionless water depth as a function of the dimensionless time $(t - T)$ where T is the passage time of the bore front. In Figure 10.10B, some pressure data recorded at 0.225 m above the bed are further included. Further details on each field study are reported in Table 10.2.

All the turbulent velocity data show a rapid deceleration of the flow associated with the passage of the bore as illustrated in Figure 10.11. Figure 10.11 shows some typical time variations of the longitudinal velocity component during the propagation of tidal bores. The data are presented in a dimensionless form based upon the momentum considerations developed above. In most natural systems, the bore passage is associated with a flow reversal ($V_x < 0$) although this might not be always the case (Bazin, 1865; Kjerfve and Ferreira, 1993). Some large fluctuations of longitudinal velocities are observed during and shortly after the bore at all vertical elevations within the water column. The tidal bore acts as

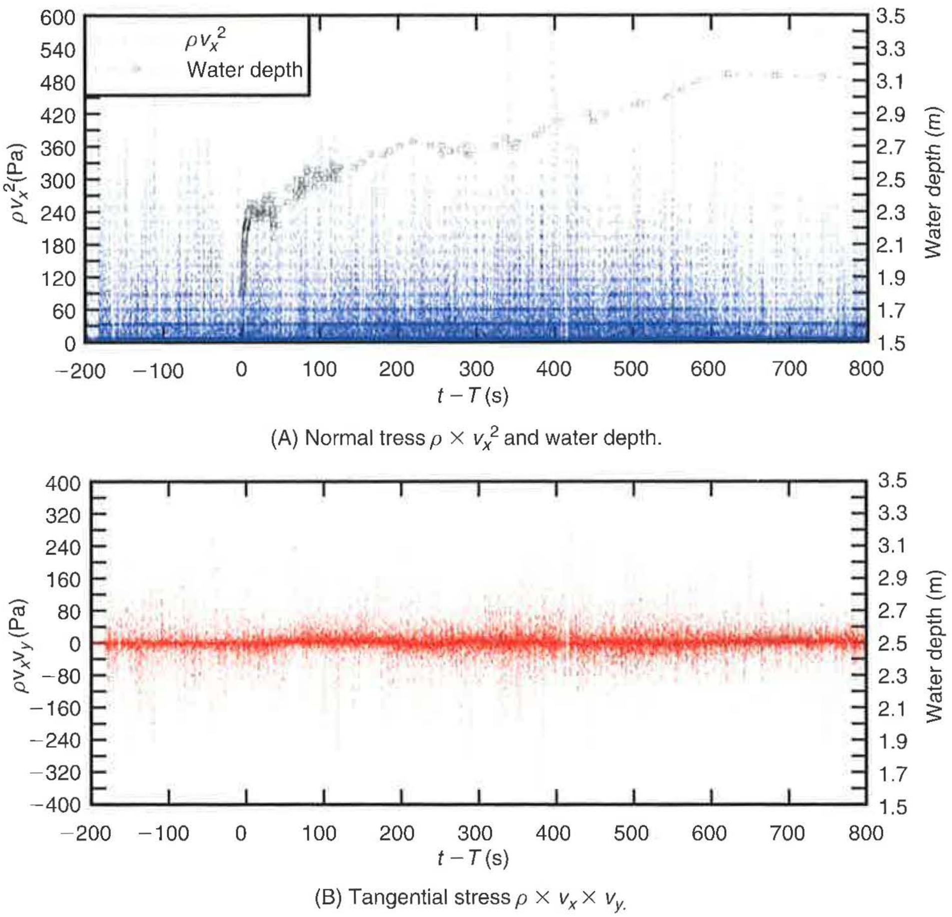

Figure 10.12. Time-variations of the turbulent Reynolds stresses during the passage of the undular tidal bore of the Garonne River on 11 September 2010.

a hydrodynamic shock with a sudden change in velocity and pressure fields. The tidal bore is always followed by some highly turbulent flow motion with long lasting effects. Both the transverse and vertical velocity component data present some large and rapid fluctuations with time immediately after the bore passage. The bore passage is further associated with some relatively-long-period oscillations superposed to some high-frequency turbulent fluctuations. The former may be linked with the formation, development and advection of large-scale coherent structures behind the front, as hinted by some recent numerical simulations (see for example Lubin *et al.*, 2010).

The unsteady turbulent flow motion is characterised by large turbulent stresses, and turbulent stress fluctuations, below the tidal bore and following whelp motion. The data indicate that the turbulent stress magnitudes are larger than in the initial turbulent flow shortly prior to the bore, and highlight the intense turbulent mixing beneath the tidal bore (Fig. 10.12). Figure 10.12 presents some results in terms of normal and tangential Reynolds stresses during an undular tidal bore; note that the results are presented in dimensional form. The instantaneous turbulent shear stress magnitudes are larger than the critical threshold for sediment motion and transport, although the comparison has some limits. In a turbulent bore, the large scale vortices play an important role in terms of sediment material pickup

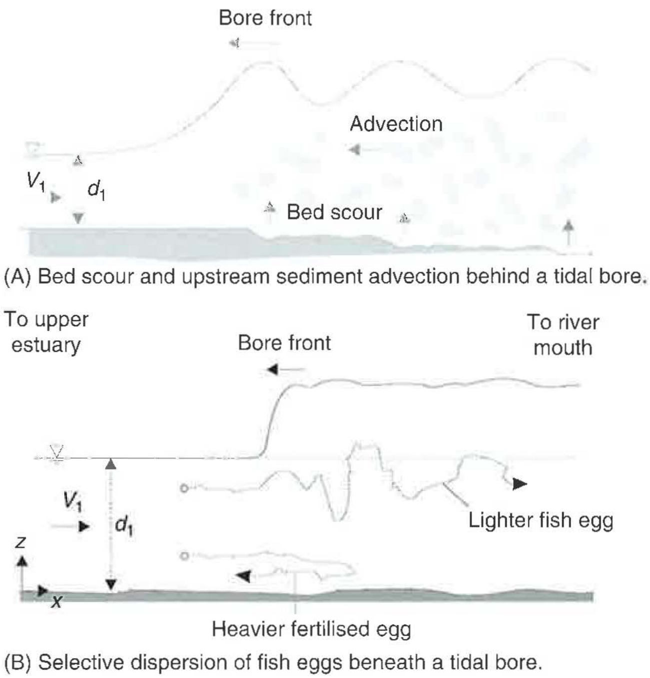

Figure 10.13. Conceptual sketches of the impact of tidal bores on estuarine systems.

and upward advection. Sediment motion occurs by convection since the turbulent length scale is much larger than the sediment characteristic size. Further the high levels of shear stresses revealed during the field measurements occur during very short transient times (turbulent bursts) rather at a continuous level like in a steady fluvial motion.

The field data illustrate that a tidal bore induces a very strong mixing in the natural channel, for which the classical mixing theories do not account for. During the tidal bore passage, and the eroded material and other scalars are advected upstream in the whelps and wave motion behind the bore front. The results are consistent with the very strong turbulent mixing observed in the tidal-bore affected estuaries, associated with the accretion and deposition of sediment materials in the upper estuarine zones.

10.3.3 Discussion

Both field measurements and laboratory studies (see bibliography) highlight some key features of the impact of tidal bores on the estuarine system.

The turbulent velocity measurements indicate the existence of energetic turbulent events during and behind the tidal bore (Fig. 10.11 & 10.12). These are highlighted by large and rapid fluctuations of turbulent velocities and Reynolds stresses. The duration of the turbulent events seem larger beneath undular bores, and shorter and more intense beneath breaking bores. This type of macro-turbulence can maintain its coherence as the eddies are advected behind the bore. Importantly the macro-turbulence contributes to significant sediment erosion from the bed and banks, and the upstream advection of the eroded material as illustrated in Figure 10.13A.

A recent study showed the preferential dispersion of fish eggs in a tidal bore affected estuary (Chanson and Tan, 2010). The fish eggs are typically advected downstream during the ebb tide. The arrival of the tidal bore induces a selective longitudinal dispersion of

(A) Tidal bore of the Sélune River on 7 April 2004 at sunrise - Bore propagation from left to right.

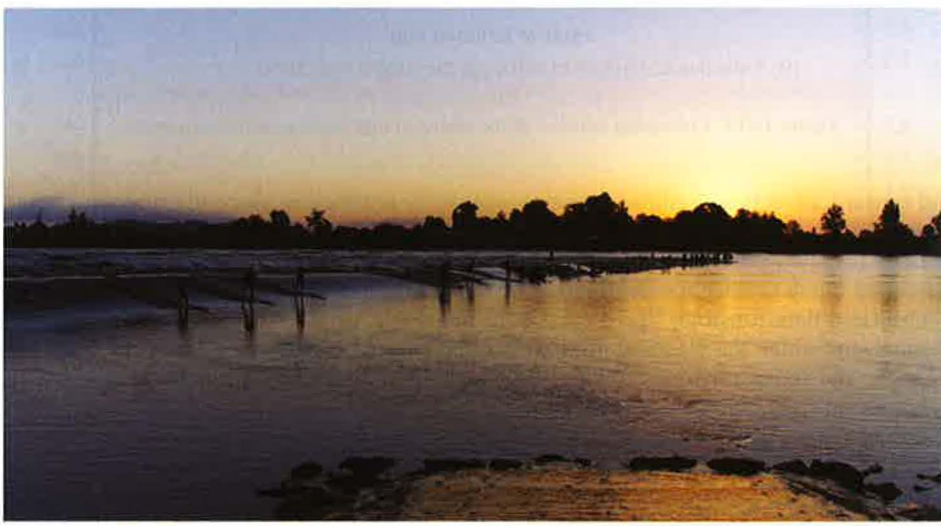

(B) Tidal bore of the Dordogne River on 12 September 2010 at sunrise - Bore propagation from left to right.

Figure 10.14. Tidal bore propagation at sunrise.

the eggs. The lightest, unfertilised fish eggs tend to flow downstream towards the river mouth, while the fertilised fish eggs are advected upstream behind the bore (Fig. 10.13B). The tidal bore induces a rapid longitudinal spread of the eggs with some preferential mixing depending upon their density and stages of development. The fertilised fish eggs are confined by the tidal bore to the upper estuary that is the known breeding grounds of juveniles. The unfertilised, neutrally buoyant eggs continue downstream possibly up to the river mouth, although the strong flood flow may bring them back into the upper estuary at a later stage of the tidal cycle. Figure 10.13B illustrates the selective dispersion process.

More generally the bore occurrence is essential to a number of ecological processes and the sustainability of unique eco-systems. The tidal bore propagation induces a massive

(A) Road sign to the benak (tidal bore) of the Batang Lupar, Sri Aman (Malaysia) (Courtesy of Antony Colas).
(B) Stamped postal envelop edited by the French Post Office in 2010 as part of a series on the tidal bores in Gironde.

(C) Tidal bore of the Qiang Tang River (China) overtopping its banks on 31August 2011 during a combination of strong spring tide as the typhoon Nanmadol approached the coastline (Photo by ChinaFotoPress/Getty Images).

Figure 10.15. Impact of tidal bores on the human society.

mixing of estuarine waters stirring the organic matter and creating some rich fishing grounds (for example, the Rokan River in Indonesia).

10.4 CONCLUSION

A tidal bore is a hydrodynamic shock propagating upstream as the tidal flow turns to rising and forming during the spring tides when the tidal range exceeds 5–6 m and the flood tide is confined to a narrow funnelled estuary with low freshwater levels. The tidal bore propagation induces a massive mixing of the natural system and its occurrence is critical to the environmental balance of the estuarine zone.

The application of continuity and momentum principles gives a complete solution of the ratio of the conjugate cross-section areas as a function of the upstream Froude number

$Fr_1 = (V_1 + U)/\sqrt{g \times A_1/B_1}$ for a range of channel cross-sections. The effects of the flow resistance are observed to decrease the ratio of conjugate depths for a given Froude number. The field observations show that the tidal bore passage is associated with large fluctuations in water depth and instantaneous velocity components associated with intense turbulent mixing. Some detailed turbulent velocity measurements at several vertical elevations during and shortly after the bore passage highlight some seminal features of tidal bores: namely some relatively-long-term oscillations in terms of flow depth and velocity superposed to some high-frequency turbulent fluctuations.

The interactions between tidal bores and human society are complex (Fig. 10.14 & 10.15). A tidal bore impacts on a range of socio-economic resources, encompassing the sedimentation of the upper estuary, the impact on the reproduction and development of native fish species, and the sustainability of unique eco-systems. A tidal bore can be a major tourism attraction like in North America, Far East Asia and Europe (Fig. 10.14 & 10.15A). A number of bores are surfed with tidal bore surfing competitions and festivals in South America, Europe and South-East Asia. But a tidal bore is a massive hydrodynamic shock which might become dangerous (Fig. 10.15C) and hinder the local traffic and development. A bore is an integral part of the environmental and socio-cultural heritage (Fig. 10.15B). It is a fascinating geophysical phenomenon in terms of geo-morphological and biological processes, as well as for the estuarine populations. Yet it remains a challenging research topic to the scientists, engineers and socio-environment experts.

ACKNOWLEDGEMENTS

The author thanks Dr Pierre Lubin, University of Bordeaux, for his valuable inputs and fruitful exchanges. He acknowledges the assistance of all the people (incl. colleagues, students, friends and relatives) who participated to the field works, and without whom this contribution could not have been possible. He thanks Dr Carlo Gualtieri for his encouragement to develop this contribution. The financial support of the University of Queensland, the Université de Bordeaux, the Australian Academy of Science and the Agence Nationale de la Recherche (Projet 10-BLAN-0911-01) is acknowledged.

APPENDIX A – LIST OF SYMBOLS

List of Symbols

Symbol	Definition	Dimensions or Units
A	cross-section area	$[L^2]$
A_1	initial cross-section area	$[L^2]$
A_2	flow cross-section area behind the bore	$[L^2]$
B	characteristic free-surface width	[L]
B'	characteristic free-surface width	[L]
B_1	upstream free-surface width	[L]
B_2	free-surface width behind the bore	[L]
d_1	upstream flow depth	[L]
d_2	flow depth behind the bore	[L]
g	gravitational acceleration constant	$[L\,T^{-2}]$
Fr	tidal bore Froude number	–

(Continued)

List of Symbols

Symbol	Definition	Dimensions or Units
Fr_1	inflow Froude number of tidal bore	–
F_{fric}	friction force	[N]
g	gravity acceleration	$[L\,T^{-2}]$
P	pressure	$[N\,m^{-2}]$
Q	water discharge	$[L^3 \cdot T^{-1}]$
T	time of tidal bore passage	[T]
t	time	[T]
Tu	turbulence intensity	–
U	tidal bore celerity positive upstream	$[L\,T^{-1}]$
V_x	longitudinal velocity component	$[L\,T^{-1}]$
V_y	transverse velocity component	$[L\,T^{-1}]$
V_z	vertical velocity component	$[L\,T^{-1}]$
V_1	initial flow velocity positive downstream	$[L\,T^{-1}]$
V_2	flow velocity behind the bore positive downstream	$[L\,T^{-}]$
W	weight force	[N]
x	longitudinal/streamwise direction	[L]
y	transverse or radial direction	[L]
z	vertical direction positive upward	[L]
β	momentum correction coefficient	–
μ	water dynamic viscosity	$[M\,L^{-1}\,T^{-1}]$
θ	angle between bed slope and horizontal	–
ρ	water density	$[M\,L^{-3}]$
σ	surface tension between air and water	$[N\,m^{-1}]$

APPENDIX B – SYNOPSIS

A tidal bore is a hydrodynamic shock propagating upstream as the tidal flow turns to rising. A tidal bore forms during the spring tides when the tidal range exceeds 5–6 m and the flood tide is confined to a narrow funnelled estuary with low freshwater levels. The tidal bore propagation induces a massive mixing of the natural system. Its occurrence is critical to the environmental balance of the estuarine zone. The application of continuity and momentum principles gives a complete solution of the ratio of the conjugate cross-section areas as a function of the upstream Froude number $Fr_1 = (V_1 + U)/\sqrt{g \times A_1/B_1}$. The flow resistance is observed to decrease the ratio of conjugate depths for a given Froude number. The tidal bore passage is associated with large fluctuations in water depth and instantaneous velocity components. This is associated with intense turbulent mixing, and sediment scour and advection in a natural system. The interactions between tidal bores and human society are complex. Both positive and adverse impacts may be encountered. Tidal bore surfing is becoming a renown extreme sport.

APPENDIX C – KEYWORDS

Tidal bore	Turbulent mixing
Momentum considerations	Froude number
Undular bores	Turbulent stresses
Breaking bores	Sediment processes
Flow resistance	Hydrodynamic shock

APPENDIX D – QUESTIONS

What are the three basic requirements for the occurrence of tidal bores?
What is the main driving mechanism of a tidal bore?
How many tidal bores are observed worldwide?
What is the basic principle used to analyse a tidal bore flow motion?
Write the tidal bore Froude number and explain each term.
What is the effect of boundary friction on the tidal bore properties?
What are the potential impacts of a tidal bore in a natural estuarine system?
Where can we see tidal bore surfing?

APPENDIX E – PROBLEMS

E1. Using tide predictions for France and China, predict the likely dates of tidal bore occurrence in the Bay of Mont Michel and in the Qiantang River in September 2013.

This may require to surf the Internet to find the tide predictions for the Bay of Mont Michel and the Qiantang River.

E2. On the 27 Sept. 2000, the flow conditions of the tidal bore of the Dordogne River were: initial water depth = 1.5 m, initial flow velocity = +0.22 m/s, observed bore celerity: 4.8 m/s. Assuming a wide rectangular channel, calculate the flow velocity after the passage of the bore. (Use the downstream flow direction as positive axis.) Numerical solution: $V_2 = -1.26$ m/s (flow reversal), $d_2 = 2.13$ m.

E3. Plot the relationship between the ratio of conjugate cross-section areas and dimensionless flow resistance force for two Garonne River data sets listed in Table 10.1. Deduce the dimensionless flow resistance force from the observations.

REFERENCES

Bazin, H. (1865). "Recherches Expérimentales sur la Propagation des Ondes." ('Experimental Research on Wave Propagation.') Mémoires présentés par divers savants à l'Académie des Sciences, Paris, France, Vol. 19, pp. 495–644 (in French).

Boussinesq, J.V. (1877). "Essai sur la Théorie des Eaux Courantes." ('Essay on the Theory of Water Flow.') Mémoires présentés par divers savants à l'Académie des Sciences, Paris, France, Vol. 23, Série 3, No. 1, supplément 24, pp. 1–680 (in French).

Chanson, H. (2004). "The Hydraulics of Open Channel Flow: An Introduction." Butterworth-Heinemann, 2nd edition, Oxford, UK, 630 pages (ISBN 978 0 7506 5978 9).

Chanson, H. (2010). "Undular Tidal Bores: Basic Theory and Free-surface Characteristics." Journal of Hydraulic Engineering, ASCE, Vol. 136, No. 11, pp. 940–944 (DOI: 10.1061/(ASCE)HY.1943-7900.0000264).

Chanson, H. (2011). "Tidal Bores, Aegir, Eagre, Mascaret, Pororoca: Theory and Observations." World Scientific, Singapore, 220 pages (ISBN 9789814335416).

Chanson, H., Lubin, P., Simon, B., and Reungoat, D. (2010). "Turbulence and Sediment Processes in the Tidal Bore of the Garonne River: First Observations." Hydraulic Model Report No. CH79/10, School of Civil Engineering, The University of Queensland, Brisbane, Australia, 97 pages.

Chanson, H., and Tan, K.K. (2010). "Turbulent Mixing of Particles under Tidal Bores: an Experimental Analysis." Journal of Hydraulic Research, IAHR, Vol. 48, No. 5, pp. 641–649 (DOI: 10.1080/00221686.2010.512779 (ISSN 0022-1686).

Darwin, G.H. (1897). The Tides and Kindred Phenomena in the Solar System." Lectures delivered at the Lowell Institute, Boston, W.H. Freeman and Co. Publ., London, 1962.

Henderson, F.M. (1966). "Open Channel Flow." MacMillan Company, New York, USA.

Kjerfve, B., and Ferreira, H.O. (1993). "Tidal Bores: First Ever Measurements." Ciência e Cultura (Jl of the Brazilian Assoc. for the Advancement of Science), Vol. 45, No. 2, March/April, pp. 135–138.

La Condamine, C.H. de (1745). "Relation abrégée d'un voyage fait dans l'intérieur de l'Amérique méridionale, depuis la côte de la mer du sud jusqu'aux côtes du Brésil et de la Guyane, en descendant la rivière des Amazones." ('Diary of the Inland Travel to Southern America, from West to East up to Brazil and Guyana, following the Amazon River.') J.E.Dufour and P. Roux Libraires, Maestricht, 415 pages (in French).

Lemoine, R. (1948). "Sur les Ondes Positives de Translation dans les Canaux et sur le Ressaut Ondulé de Faible Amplitude." ('On the Positive Surges in Channels and on the Undular Jumps of Low Wave Height.') Jl La Houille Blanche, Mar–Apr., pp. 183–185 (in French).

Leutheusser, H.J., and Schiller, E.J. (1975). "Hydraulic Jump in a Rough Channel." Water Power & Dam Construction, Vol. 27, No. 5, pp. 186–191.

Liggett, J.A. (1994). "Fluid Mechanics." McGraw-Hill, New York, USA.

Lighthill, J. (1978). "Waves in Fluids." Cambridge University Press, Cambridge, UK, 504 pages.

Lubin, P., Glockner, S., and Chanson, H. (2010). "Numerical Simulation of a Weak Breaking Tidal Bore." Mechanics Research Communications, Vol. 37, No. 1, pp. 119–121 (DOI: 10.1016/j.mechrescom.2009.09.008).

Moore, R.N. (1888). "Report on the Bore of the Tsien-Tang Kiang." Hydrographic Office, London.

Mouazé, D., Chanson, H., and Simon, B. (2010). "Field Measurements in the Tidal Bore of the Sélune River in the Bay of Mont Saint Michel (September 2010)." Hydraulic Model Report No. CH81/10, School of Civil Engineering, The University of Queensland, Brisbane, Australia, 72 pages

Moule, A.C. (1923). "The Bore on the Ch'ien-T'ang River in China." T'oung Pao, Archives pour servir à l'étude de l'histoire, des langues, la geographie et l'ethnographie de l'Asie Orientale (Chine, Japon, Corée, Indo-Chine, Asie Centrale et Malaisie), Vol. 22, pp. 10–188.

Rayleigh, Lord (1908). "Note on Tidal Bores." Proc. Royal Soc. of London, Series A containing Papers of a Mathematical and Physical Character, Vol. 81, No. 541, pp. 448–449.

Simpson, J.H., Fisher, N.R., and Wiles, P. (2004). "Reynolds Stress and TKE Production in an Estuary with a Tidal Bore." Estuarine, Coastal and Shelf Science, Vol. 60, No. 4, pp. 619–627.

Wolanski, E., Williams, D., Spagnol, S., and Chanson, H. (2004). "Undular Tidal Bore Dynamics in the Daly Estuary, Northern Australia." Estuarine, Coastal and Shelf Science, Vol. 60, No. 4, pp. 629–636 (DOI: 10.1016/j.ecss.2004.03.001).

Bibliography: tidal bore research at the University of Queensland

Reviews

Chanson, H. (2004). "Mixing and Dispersion Role of Tidal Bores." in "Fluvial, Environmental & Coastal Developments in Hydraulic Engineering", Balkema, Leiden, The Netherlands, Proc. Intl Workshop on State-of-the-Art Hydraulic Engineering, 16–19 Feb. 2004, Bari, Italy, M. Mossa, Y. Yasuda and H. Chanson Ed., pp. 223–232.

Chanson, H. (2005). "Mascaret, Aegir, Pororoca, Tidal Bore. Quid ? Où? Quand? Comment? Pourquoi ?" Jl La Houille Blanche, No. 3, pp. 103–114 (in French).

Chanson, H. (2009). "Environmental, Ecological and Cultural Impacts of Tidal Bores, Benaks, Bonos and Burros." Proc. International Workshop on Environmental Hydraulics IWEH09, Theoretical, Experimental and Computational Solutions, Valencia, Spain, 29–30 Oct., P.A. Lopez-Jimenez, V.S. Fuertes-Miquel, P.L. Iglesias-Rey, G. Lopez-Patino, F.J. Martinez-Solano, and G. Palau-Selvador Eds., Invited keynote lecture, 20 pages (CD-ROM).

Chanson, H. (2010). "Tidal Bores, Aegir and Pororoca: the Geophysical Wonders." Proc. of 17th Congress of IAHR Asia and Pacific Division, IAHR-APD, Auckland, New Zealand, 21–24 Feb., B. Melville, G. De Costa, and T. Swann Eds., Invited keynote lecture, 18 pages.

Chanson, H. (2010). "Undular Bores." Proc. Second International Conference on Coastal Zone Engineering and Management (Arabian Coast 2010), November 1–3, 2010, Muscat, Oman, Invited plenary lecture, 12 pages.

Chanson, H. (2011). "Current Knowledge in Tidal bores and their Environmental, Ecological and Cultural Impacts." Environmental Fluid Mechanics, Vol. 11, No. 1, pp. 77–98 (DOI: 10.1007/s10652-009-9160-5)

Theoretical analyses

Chanson, H. (2010). "Undular Tidal Bores: Basic Theory and Free-surface Characteristics." Journal of Hydraulic Engineering, ASCE, Vol. 136, No. 11, pp. 940–944 (DOI: 10.1061/(ASCE)HY.1943-7900.0000264).

Chanson, H. (2012). "Momentum Considerations in Hydraulic Jumps and Bores." Journal of Irrigation and Drainage Engineering, ASCE, Vol. 138 (DOI: 10.1061/(ASCE)IR.1943-4774.0000409). [In Print].

Field observations

Chanson, H. (2001). "Flow Field in a Tidal Bore: a Physical Model." Proc. 29th IAHR Congress, Beijing, China, Theme E, Tsinghua University Press, Beijing, G. LI Ed., pp. 365–373. (CD-ROM, Tsinghua University Press, ISBN 7-900637-10-9.)

Chanson, H. (2004). "Coastal Observations: The Tidal Bore of the Sélune River, Mont Saint Michel Bay, France." Shore & Beach, Vol. 72, No. 4, pp. 14–16.

Chanson, H. (2005). "Tidal Bore Processes in the Baie du Mont Saint Michel (France): Field Observations and Discussion." Proc. 31st Biennial IAHR Congress, Seoul, Korea, B.H. Jun, S.I. Lee, I.W. Seo and G.W. Choi Editors, Theme E.4, Paper 0062, pp. 4037–4046.

Chanson, H. (2008). "Photographic Observations of Tidal Bores (Mascarets) in France." Hydraulic Model Report No. CH71/08, Div. of Civil Engineering, The University of Queensland, Brisbane, Australia, 104 pages, 1 movie and 2 audio files (ISBN 9781864999303).

Chanson, H. (2009). "The Rumble Sound Generated by a Tidal Bore Event in the Baie du Mont Saint Michel." Journal of Acoustical Society of America, Vol. 125, No. 6, pp. 3561–3568 (DOI: 10.1121/1.3124781).

Chanson, H., Lubin, P., Simon, B., and Reungoat, D. (2010). "Turbulence and Sediment Processes in the Tidal Bore of the Garonne River: First Observations." Hydraulic Model Report No. CH79/10, School of Civil Engineering, The University of Queensland, Brisbane, Australia, 97 pages.

Chanson, H. Reungoat, D., Simon, B., and Lubin, P. (2011). "High-Frequency Turbulence and Suspended Sediment Concentration Measurements in the Garonne River Tidal Bore." Estuarine Coastal and Shelf Science, Vol. 95, No. 2–3, pp. 298–306 (DOI 10.1016/j.ecss.2011.09.012)

Mouaze, D., Chanson, H., and Simon, B. (2010). "Field Measurements in the Tidal Bore of the Sélune River in the Bay of Mont Saint Michel (September 2010)." Hydraulic Model Report No. CH81/10, School of Civil Engineering, The University of Queensland, Brisbane, Australia, 72 pages (ISBN 9781742720210).

Simon, B., Lubin, P., Reungoat, D., and Chanson, H. (2011). "Turbulence Measurements in the Garonne River Tidal Bore: First Observations." Proc. 34th IAHR World Congress, Brisbane, Australia, 26 June–1 July, Engineers Australia Publication, Eric Valentine, Colin Apelt, James Ball, Hubert Chanson, Ron Cox, Rob Ettema, George Kuczera, Martin Lambert, Bruce Melville and Jane Sargison Editors, pp. 1141–1148.

Physical studies

Chanson, H. (2001). "Flow Field in a Tidal Bore : a Physical Model." Proc. 29th IAHR Congress, Beijing, China, Theme E, Tsinghua University Press, Beijing, G. LI Ed., pp. 365–373. (CD-ROM, Tsinghua University Press, ISBN 7-900637-10-9.)

Chanson, H. (2005). "Physical Modelling of the Flow Field in an Undular Tidal Bore." Jl of Hyd. Res., IAHR, Vol. 43, No. 3, pp. 234–244.

Chanson, H. (2008). "Turbulence in Positive Surges and Tidal Bores. Effects of Bed Roughness and Adverse Bed Slopes." Hydraulic Model Report No. CH68/08, Div. of Civil Engineering, The University of Queensland, Brisbane, Australia, 121 pages & 5 movie files (ISBN 9781864999198).

Chanson, H. (2009). "An Experimental Study of Tidal Bore Propagation: the Impact of Bridge Piers and Channel Constriction." Hydraulic Model Report No. CH74/08, School of Civil Engineering, The University of Queensland, Brisbane, Australia, 110 pages & 5 movie files (ISBN 9781864999600).

Chanson, H. (2010). "Undular Tidal Bores: Basic Theory and Free-surface Characteristics." Journal of Hydraulic Engineering, ASCE, Vol. 136, No. 11, pp. 940–944 (DOI: 10.1061/(ASCE)HY.1943-7900.0000264).

Chanson, H. (2010). "Unsteady Turbulence in Tidal Bores: Effects of Bed Roughness." Journal of Waterway, Port, Coastal, and Ocean Engineering, ASCE, Vol. 136, No. 5, pp. 247–256 (DOI: 10.1061/(ASCE)WW.1943-5460.0000048).

Chanson, H. (2011). "Undular Tidal Bores: Effect of Channel Constriction and Bridge Piers." Environmental Fluid Mechanics, Vol. 11, No. 4, pp. 385–404 & 4 videos (DOI: 10.1007/s10652-010-9189-5).

Chanson, H. (2011). "Turbulent Shear Stresses in Hydraulic Jumps and Decelerating Surges: An Experimental Study." Earth Surface Processes and Landforms, Vol. 36, No. 2, pp. 180–189 & 2 videos (DOI: 10.1002/esp.2031).

Chanson, H., and Docherty, N.J. (2010). "Unsteady Turbulence in Tidal Bores: Ensemble-Average or VITA?" Proc. 17th Australasian Fluid Mechanics Conference, Auckland, New Zealand, 5–9 Dec., 4 pages.

Chanson, H., and Docherty, N.J. (2012). "Turbulent Velocity Measurements in Open Channel Bores." European Journal of Mechanics B/Fluids, Vol. 31 (DOI 10.1016/j.euromechflu.2011.10.001). [In Print].

Chanson, H., and Tan, K.K. (2010). "Particle Dispersion under Tidal Bores: Application to Sediments and Fish Eggs." Proc. 7th International Conference on Multiphase Flow ICMF 2010, Tampa FL, USA, May 30–June 4, Paper No. 12.7.3, 9 pages (USB Memory Stick).

Chanson, H., and Tan, K.K. (2010). "Turbulent Mixing of Particles under Tidal Bores: an Experimental Analysis." Journal of Hydraulic Research, IAHR, Vol. 48, No. 5, pp. 641–649 (DOI: 10.1080/00221686.2010.512779 (ISSN 0022–1686).

Chanson, H., and Tan, K.K. (2011). "Dispersion of Fish Eggs under Undular and Breaking Tidal Bores." Fluid Dynamics & Materials Processing, Vol. [In Print].

Docherty, N.J., and Chanson, H. (2010). "Characterisation of Unsteady Turbulence in Breaking Tidal Bores including the Effects of Bed Roughness." Hydraulic Model Report No. CH76/10, School of Civil Engineering, The University of Queensland, Brisbane, Australia, 112 pages.

Docherty, N.J., and Chanson, H. (2011). "Unsteady Turbulence Measurements in Breaking Tidal Bores including the Effect of Bed Roughness." Proc. 34th IAHR World Congress, Brisbane, Australia, 26 June–1 July, Engineers Australia Publication, Eric Valentine, Colin Apelt, James Ball, Hubert Chanson, Ron Cox, Rob Ettema, George Kuczera, Martin Lambert, Bruce Melville and Jane Sargison Editors, pp. 1039–1046.

Donnelly, C., and Chanson, H. (2005). "Environmental Impact of Undular Tidal Bores in Tropical Rivers." Environmental Fluid Mechanics, Vol. 5, No. 5, pp. 481–494 (DOI: 10.1007/s10652-005-0711-0).

Gualtieri, C., and Chanson, H. (2011). "Hydrodynamics and Turbulence in Positive Surges. A Comparative Study." Proc. 34th IAHR World Congress, Brisbane, Australia, 26 June–1 July, Engineers Australia Publication, Eric Valentine, Colin Apelt, James Ball, Hubert Chanson, Ron Cox, Rob Ettema, George Kuczera, Martin Lambert, Bruce Melville and Jane Sargison Editors, pp. 1062–1069.

Khezri, N., and Chanson, H. (2011). "Inception of Gravel Bed Motion beneath Tidal Bores: an Experimental Study." Proc. 34th IAHR World Congress, Brisbane, Australia, 26 June–1 July, Engineers Australia Publication, Eric Valentine, Colin Apelt, James Ball, Hubert Chanson, Ron Cox, Rob Ettema, George Kuczera, Martin Lambert, Bruce Melville and Jane Sargison Editors, pp. 1077–1084.

Koch, C., and Chanson, H. (2005). "An Experimental Study of Tidal Bores and Positive Surges: Hydrodynamics and Turbulence of the Bore Front." Report No. CH56/05, Dept. of Civil Engineering, The University of Queensland, Brisbane, Australia, July, 170 pages (ISBN 978-1-86499-824-5).

Koch, C., and Chanson, H. (2008). "Turbulent Mixing beneath an Undular Bore Front." Journal of Coastal Research, Vol. 24, No. 4, pp. 999–1007 (DOI: 10.2112/06-0688.1).

Koch, C., and Chanson, H. (2009). "Turbulence Measurements in Positive Surges and Bores." Journal of Hydraulic Research, IAHR, Vol. 47, No. 1, pp. 29–40 (DOI: 10.3826/jhr.2009.2954).

Numerical modelling

Chanson, H., Lubin, P., and Glockner, S. (2011). "Unsteady Turbulence in a Shock: Physical and Numerical Modelling in Tidal Bores and Hydraulic Jumps." in "Turbulence: Theory, Types and Simulation", Nova Science Publishers, Hauppauge NY, USA. [In Print].

Furuyama, S., and Chanson, H. (2008). "A Numerical Study of Open Channel Flow Hydrodynamics and Turbulence of the Tidal Bore and Dam-Break Flows." Report No. CH66/08, Div. of Civil Engineering, The University of Queensland, Brisbane, Australia, May, 88 pages (ISBN 9781864999068).

Furuyama, S., and Chanson, H. (2010). "A Numerical Solution of a Tidal Bore Flow." Coastal Engineering Journal, Vol. 52, No. 3, pp. 215–234 (DOI: 10.1142/S057856341000218X).

Lubin, P., Glockner, S., and Chanson, H. (2010). "Numerical Simulation of a Weak Breaking Tidal Bore." Mechanics Research Communications, Vol. 37, No. 1, pp. 119–121 (DOI: 10.1016/j.mechrescom.2009.09.008).

Lubin, P., Chanson, H., and Glockner, S. (2010). "Large Eddy Simulation of Turbulence Generated by a Weak Breaking Tidal Bore." Environmental Fluid Mechanics, Vol. (DOI: 10.1007/s10652-009-9165-0).

Reichstetter, M., and Chanson, H. (2011). "Negative Surge in Open Channel: Physical, Numerical and Analytical Modelling." Proc. 34th IAHR World Congress, Brisbane, Australia, 26 June–1 July, Engineers Australia Publication, Eric Valentine, Colin Apelt, James Ball, Hubert Chanson, Ron Cox, Rob Ettema, George Kuczera, Martin Lambert, Bruce Melville and Jane Sargison Editors, pp. 2306–2313.

Simon, B., Lubin, P., Glockner, S., and Chanson, H. (2011). "Three-Dimensional Numerical Simulation of the Hydrodynamics generated by a Weak Breaking Tidal Bore." Proc. 34th IAHR World Congress, Brisbane, Australia, 26 June–1 July, Engineers Australia Publication, Eric Valentine, Colin Apelt, James Ball, Hubert Chanson, Ron Cox, Rob Ettema, George Kuczera, Martin Lambert, Bruce Melville and Jane Sargison Editors, pp. 1133–1140.

Internet resources

Chanson, H. (2000). "The Tidal Bore of the Seine River, France." Internet resource (Internet address: http://www.uq.edu.au/~e2hchans/mascaret.html).

Chanson, H., (2003). "Free-surface undulations in open channel flows: Undular jumps, Undular bores, Standing waves." Internet resource (Internet address: http://www.uq.edu.au/~e2hchans/undular.html).

Chanson, H. (2004). "Tidal bores, Mascaret, Pororoca. Myths, Fables and Reality !!!." Internet resource (Internet address: http://www.uq.edu.au/~e2hchans/tid_bore.html).

Open access research reprints on tidal bores (Internet address: http://espace.library.uq.edu.au/list/author_id/193/).

Audio-visual resources

Chanson, H. (2005). "Tidal Bore of the Dordogne River (France) on 27 September 2000." Flowvis: the Art of Fluid Dynamics, Australian Institute of Physics' (AIP) "Physics for the Nation" Congress, Australian National University (ANU), School of Art, Canberra, Australia, 31 Jan. to 4 Feb. 2005.

Lespinasse, M. (2004). "La Tribu du Mascaret" ('Surfing the Dordogne') Grand Angle production, France, 30 minutes.

Lespinasse, M. (2005). "Les Fils de la Lune" ('The Children of the Moon') Grand Angle production, France, 50 minutes.

Lespinasse, M. (2008). "Rendez Vous avec le Dragon" ('Appointment with the Dragon') Thalassa, France, 30 minutes.

NHK Japan Broadcasting Corp (1989). "Pororoca: the Backward Flow of the Amazon." Videocassette VHS colour, NHK, Japan, 29 minutes.

CRC Press / Balkema
Taylor & Francis Group

About the Editors

Carlo Gualtieri is currently Assistant Professor in Environmental Hydraulics at the Civil, Construction and Environmental Engineering Department (DICEA) (formerly Hydraulic, Geotechnical and Environmental Engineering Department) of the University of Napoli Federico II. At the same university he received a B.Sc. in Hydraulic Engineering, a M.Sc. in Environmental Engineering and a Ph.D. in Environmental Engineering. He was Visiting Academic at the University of Queensland, Australia, and Guest lecturer at the Eindhoven University of Technology, The Netherlands. Since 2006 he is a member of the Editorial Board of *Environmental Modelling and Software* (Elsevier) and since 2008 of *Environmental Fluid Mechanics* (Springer).

Dragutin T. Mihailović is Professor of Meteorology and Biophysics at the Department of Vegetable and Crops, Faculty of Agriculture, University of Novi Sad, Serbia. He is also Professor of Modelling Physical Processes at the Department of Physics, Faculty of Sciences at the same university and Visiting Professor at the State University of New York at Albany, NY (USA). He received a B.Sc. in Physics at the University of Belgrade, Serbia, his M.Sc. in Dynamic Meteorology at the University of Belgrade. He is head of the Center for Meteorology and Environmental Modelling (CMEM) of the University of Novi Sad where he has teaching activities. He is also head of the Center for Meteorology and Environmental Predictions, Department of Physics, Faculty of Sciences, University of Novi Sad.

Fluid Mechanics of Environmental Interfaces

Second Edition

Editors:
Carlo Gualtieri
Dragutin T. Mihailović

CRC Press
Taylor & Francis Group
A BALKEMA BOOK

CRC Press / Balkema
Taylor & Francis Group

Fluid Mechanics of Environmental Interfaces

Second Edition

Edited by **Carlo Gualtieri**, *University of Napoli Federico II, Napoli, Italy* & **Dragutin T. Mihailović**, *University of Novi Sad, Novi Sad, Serbia*

Environmental Fluid Mechanics (EFM) studies the motion of air and water at several different scales, the fate and transport of species carried along by these fluids, and the interactions among those flows and geological, biological, and engineered systems. EFM emerged some decades ago as a response to the need for tools to study problems of flow and transport in rivers, estuaries, lakes, groundwater and the atmosphere; it is a topic of increasing importance for decision makers, engineers, and researchers alike.

The second edition of the successful textbook "Fluid Mechanics of Environmental Interfaces" is still aimed at providing a comprehensive overview of fluid mechanical processes occurring at the different interfaces existing in the realm of EFM, such as the air-water interface, the air-land interface, the water-sediment interface, the surface water-groundwater interface, the water-vegetation interface, and the water-biological systems interface. Across any of these interfaces mass, momentum, and heat are exchanged through different fluid mechanical processes over various spatial and temporal scales. In this second edition, the unique feature of this book, considering all the topics from the point of view of the concept of environmental interface, was maintained while the chapters were updated and five new chapters (8, 9, 10, 13 and 16) have been added to significantly enlarge the coverage of the subject area.

- ***Takes a novel approach, that is the discussion of the processes of mass, momentum, and heat exchange at various environmental interfaces***
- ***Supplies updates and five new chapters***
- ***Brings together researchers with many years of experience in the topics covered***

The book will be of interest to graduate students and researchers in environmental sciences, civil engineering and environmental engineering, (geo)physics, atmospheric science, meteorology, limnology, oceanography, and applied mathematics.

Fluid Mechanics of Environmental Interfaces, Second Edition
Edited by Carlo Gualtieri & Dragutin T. Mihailović
November 2012: 246 x 174 mm: 500 pp.
Hardback: ISBN 978-0-415-62156-4: £82.00 / $139.95
Orders, information: www.crcpress.com/9780415621564

CRC Press / Balkema
Taylor & Francis Group

Selected Contents

Part one – Preliminaries

1. Environmental fluid mechanics: Current issues and future outlook, *B. Cushman-Roisin, C. Gualtieri & D.T. Mihailović*

Part two – Processes at atmospheric interfaces

2. Point source atmospheric diffusion, *B. Rajković, I. Arsenić & Z. Grsić*
3. Air–sea interaction, *V. Djurdjević & B. Rajković*
4. Modelling of flux exchanges between heterogeneous surfaces and atmosphere, *D.T. Mihailović & D. Kapor*
5. Desert dust uptake-transport and deposition mechanisms – impacts of dust on radiation, clouds and precipitation, *G. Kallos, P. Katsafados & C. Spyrou*

Part three – Processes at water interfaces

6. Gas-transfer at unsheared free-surfaces, *C. Gualtieri & G. Pulci Doria*
7. Advective diffusion of air bubbles in turbulent water flows, *H. Chanson*
8. Exchanges at the bed sediments-water column interface, *F.A. Bombardelli & P.A. Moreno* (NEW)
9. Surface water and streambed sediment interaction: The hyporheic exchange, *D. Tonina* (NEW)
10. Environmental fluid dynamics of tidal bores: Theoretical considerations and field observations, *H. Chanson* (NEW)

Part four – Processes at interfaces of biotic systems

11. Transport processes in the soil-vegetation-lower atmosphere system, *D.T. Mihailović*
12. Turbulence and wind above and within the forest canopy, *B. Lalic & D.T. Mihailović*
13. Flow and mass transport in vegetated surface waters, *Y. Tanino* (NEW)
14. Uniform flow and boundary layers over rigid vegetation, *P. Gualtieri & G. Pulci Doria*
15. Mass transport in aquatic environments, *G. Nishihara & J.D. Ackerman*
16. Maps serving as the combined coupling between interacting environmental interfaces and their behavior in the presence of dynamical noise, *D.T. Mihailović & I. Balaž* (NEW)

To order: www.crcpress.com/9780415621564

You can also place a written order with us by post, fax or e-mail:
Taylor & Francis Customer Services, c/o Bookpoint Limited
130 Milton Park, Abingdon, Oxon OX14 4SB, UNITED KINGDOM
Tel: +44 1235 400524 - Fax: +44 1235 400525 - Email: tandf@bookpoint.co.uk

For orders in the USA, Canada, Central & South America:
Broken Sound Parkway, NW, (Suite 300), Boca Raton, FL 33487, USA
Tel: 1 (800) 272 7737 - Fax: 1 (800) 374 3401 - E-mail: orders@taylorandfrancis.com

CRC Press / Balkema W: www.crcpress.com E: pub.nl@taylorandfrancis.com T: +31 71 524 3080